

# Lawrence Berkeley National Laboratory

## Recent Work

### Title

PHASE CONTOURS OF SCATTERING AMPLITUDES III HIGH ENERGY BEHAVIOR AT FIXED ANGLES

### Permalink

<https://escholarship.org/uc/item/7w3075jq>

### Authors

Eden, Richard J.  
Tan, Chung-I.

### Publication Date

1967-12-19

cy. 2

# University of California Ernest O. Lawrence Radiation Laboratory

PHASE CONTOURS OF SCATTERING AMPLITUDES III  
HIGH ENERGY BEHAVIOR AT FIXED ANGLES

Richard J. Eden and Chung-I Tan

December 19, 1967

RECEIVED  
LAWRENCE  
RADIATION LABORATORY  
LIBRARY AND  
DOCUMENTS SECTION

### TWO-WEEK LOAN COPY

This is a Library Circulating Copy  
which may be borrowed for two weeks.  
For a personal retention copy, call  
Tech. Info. Division, Ext. 5545

UCRL-17923

cy. 2

## **DISCLAIMER**

This document was prepared as an account of work sponsored by the United States Government. While this document is believed to contain correct information, neither the United States Government nor any agency thereof, nor the Regents of the University of California, nor any of their employees, makes any warranty, express or implied, or assumes any legal responsibility for the accuracy, completeness, or usefulness of any information, apparatus, product, or process disclosed, or represents that its use would not infringe privately owned rights. Reference herein to any specific commercial product, process, or service by its trade name, trademark, manufacturer, or otherwise, does not necessarily constitute or imply its endorsement, recommendation, or favoring by the United States Government or any agency thereof, or the Regents of the University of California. The views and opinions of authors expressed herein do not necessarily state or reflect those of the United States Government or any agency thereof or the Regents of the University of California.

Submitted to Physical Review

UCRL-17923  
Preprint

UNIVERSITY OF CALIFORNIA  
Lawrence Radiation Laboratory  
Berkeley, California

AEC Contract No. W-7405-eng-48

PHASE CONTOURS OF SCATTERING AMPLITUDES III  
HIGH ENERGY BEHAVIOR AT FIXED ANGLES

Richard J. Eden and Chung-I Tan

December 19, 1967

PHASE CONTOURS OF SCATTERING AMPLITUDES III  
HIGH ENERGY BEHAVIOR AT FIXED ANGLES\*

Richard J. Eden<sup>†</sup> and Chung-I Tan

Lawrence Radiation Laboratory  
University of California  
Berkeley, California

December 19, 1967

ABSTRACT

The method of phase contours is applied to some problems concerned with scattering at fixed angles. The crossing symmetric generalized Regge model developed in a previous paper is used to illustrate possible characteristics of the behavior of scattering amplitudes. These characteristics are discussed both in the complex energy plane at fixed angle and in the complex  $\cos \theta$  plane at fixed high energy. The former leads to a procedure for studying fixed angle behavior by means of entire functions on whose orders some limits can be established. The latter leads to a generalization of the lower bounds on high energy behavior obtained earlier by Cerulus and Martin, and by Chiu and Tan.

## 1. INTRODUCTION

Our main purpose in this paper is to show how the method of phase contours can be used in the problem of fixed angle scattering at high energy. In particular we will show that it gives a new way of formulating the problem, which is relevant to an heuristic approach and may also be used for a rigorous discussion of assumptions and consequent bounds on the high energy behavior.

We will make extensive use of results and techniques on phase contours that were developed in the two previous papers<sup>1,2</sup> (hereafter denoted by I and II). In particular, we will use the crossing symmetric model developed in II as a basis for formulating our discussion of fixed angle behavior. This model is based on dominance by Regge pole terms that correspond to rising trajectories. We use our knowledge of phase contours and zeros in this model to indicate the kind of behavior that should be taken into account in a more general discussion of high energy behavior at fixed angles. Two essentially different approaches are considered. The first is directed towards the use of entire functions to describe the main features of scattering at a fixed angle. The second approach makes use of modulus contours in the complex  $\cos \theta$  plane at high energy and can be used to obtain a fixed angle lower bound.

In Section 2 we express the scattering amplitude for our model at fixed momentum transfer in terms of a Herglotz function and a ratio

of polynomials in the energy. These polynomials are related to zeros of the scattering amplitude on the physical sheet and to phase contours on the boundary of the physical sheet. In Section 3 this result is generalized to fixed angle behavior, where the polynomials become replaced by entire functions. The orders of the entire functions can be related to the distribution of zeros and the distribution of phase contours. If the entire function giving the zeros is dominant at high energies, then its order must be greater than or equal to one half.

In Section 4 we study the behavior of modulus contours for the amplitude in the complex  $\cos(\theta_t)$  plane, where  $\theta_t$  is the scattering angle. By considering the limiting form of these contours at high energy in our model we see that polynomial boundedness in energy will in general be limited to a finite part of the  $\cos \theta_t$  plane. This indicates the need for a generalization of the method for obtaining lower bounds that was first developed by Cerulus and Martin. The generalization is described in Section 5.

## 2. PHASE CONTOURS FOR A CROSSING SYMMETRIC MODEL

In paper II we developed solutions for phase contours from a Regge model that satisfies certain consistency tests under crossing symmetry. The starting point for the model is the assumption that the (equal mass boson) scattering amplitude has the asymptotic form, as  $s \rightarrow +\infty$ ,

$$F(s,t) \sim \frac{b(t) s^{\alpha(t)} \exp\left[i\pi\left\{1 - \frac{1}{2}\alpha(t)\right\}\right]}{\sin\left[\frac{1}{2}\pi\alpha(t)\right] \Gamma[\alpha(t)]}. \quad (2.1)$$

In our model we assume that the Regge trajectory  $\alpha(t)$  rises continuously as  $t$  increases, and falls as  $t$  decreases. We also assume single pole dominance in the asymptotic limit  $s \rightarrow +\infty$  for fixed  $t$ , except at zeros of the residue, that come from poles of the gamma function at

$$\alpha(t) = -(2n + 1). \quad (2.2)$$

There are two essentially different types of behavior for crossing symmetric phase contours on the physical sheet that depend on the relative behavior of the leading Regge pole (2.1) and the next Regge pole. These two types of behavior were denoted (a) and (b) in Section 5 of II. We will find that with type (a) there is an infinite sequence of zeros on the physical sheet at fixed angles, whereas with type (b) this sequence of zeros of the scattering amplitude lies on



unphysical sheets. There may be mixtures of the two types but, in order to avoid an unduly long discussion, we will limit ourselves to the unmixed types.

In this section we will describe the characteristics of the phase contours in our model at fixed momentum transfer, and will use them to relate the scattering amplitude to a Herglotz function. In Section 3 we make the analagous steps at fixed angle.

#### The Phase Contours

The phase  $\phi(s,t)$ , of the scattering amplitude  $F(s,t)$ , is defined by

$$\phi(s,t) = \text{Im}[\log\{F(s,t)\}], \quad (2.3)$$

together with a specification of the route to the point  $(s,t)$  from the asymptotic forward direction, where we define our initial phase,

$$\phi(s \rightarrow \infty, t = 0) = \frac{1}{2} \pi. \quad (2.4)$$

An account of theoretical and experimental properties of phase contours was given in I. Using these properties we developed the crossing symmetric solutions of types (a) and (b) in II (Sections 5 and 7), based on Eq. (2.1) above. We will discuss case (b) first since it is somewhat simpler than (a).

Case (b)

The phase contours in the real  $s$ , real  $t$ , plane for type (b) are shown in Fig. 2.1 [see Fig. 7.1 of II]. The important features are (1) the phase oscillates between  $\pi$  and  $2\pi$  in the region

$$u > 4m^2, \quad t > 4m^2. \quad (2.5)$$

(2) the phase in the region,

$$u < 0, \quad t < 0, \quad (2.6)$$

increases as  $s$  increases. For fixed negative  $t$  and large  $s$ , its approximate value is

$$\phi(s,t) \approx \pi[1 - \alpha(t)]. \quad (2.7)$$

The correction term has magnitude less than  $\frac{1}{2}\pi$ . The difference between this phase (2.7) and the phase in the exponent in Eq. (2.1) is due to the zeros of the residue and the effects of the next highest Regge trajectory. The relation between the phase contours shown in Fig. 2.1 and the high energy behavior for fixed negative  $t$  has been discussed in II (Section 5). We will be concerned with the corresponding relation at fixed angle. However it is useful to note first some features that apply to the simpler case of fixed  $t$ .

In Fig. 2.1, the small black circles denote real zeros of the amplitude, and the attached dotted curves denote complex zeros. In

case (b), which we are now considering, these zeros remain on the physical sheet, in the complex  $s$  plane, as  $t$  decreases through real values. In addition zeros come in from infinity, each time  $t$  decreases through a zero of the residue given by a solution of Eq. (2.2). These zeros also remain on the physical sheet as  $t$  decreases.

We consider the behavior of  $F(s,t)$ , for some fixed real negative value of  $t$ , as a function of  $s$ . There will be a finite number of zeros in  $\text{Im } s > 0$ , at

$$a_1(t), a_2(t), a_3(t), \dots, a_\ell(t). \quad (2.8)$$

These can be factored out from  $F$ , giving

$$F(s,t) = \prod_1^\ell (s - a_r) G(s,t). \quad (2.9)$$

The function  $G(s,t)$  will have phase contours that determine the oscillations through zero of  $\text{Im } G(s,t)$ . Let the zeros of  $\text{Im } G(s,t)$  for real  $s$  (along  $s + i0$ ) occur at

$$b_1(t), b_2(t), \dots, b_m(t), \quad (2.10)$$

and at

$$c_1(t), c_2(t), \dots, c_n(t), \quad (2.11)$$

where  $b_i(t)$  denote points at which the phase of  $G$  increases through a value  $N_0\pi$  as  $s$  increases, and  $c_j(t)$  denotes points at which it

-7-

decreases. Then, as described in I (Sections 2 and 4), we can write  $G(s,t)$  in the form

$$G(s,t) = \frac{\prod_{i=1}^m (s - b_i)}{\prod_{j=1}^n (s - c_j)} H(s,t), \quad (2.12)$$

where  $H$  is a Herglotz function of  $s$ , and satisfies

$$\frac{C}{|s|} < |H(s,t)| < C'|s|, \quad (2.13)$$

for some  $C$  and  $C'$  as  $s \rightarrow \infty$ , in  $\text{Im } s > 0$ .

The scattering amplitude  $F$  can therefore be written in the form,

$$F(s,t) = \frac{P_a(s)P_b(s)}{P_c(s)} H(s,t), \quad (2.14)$$

where  $P_a, P_b, P_c$  denote polynomials whose order and coefficients depend on the chosen real value of  $t$ . In our model, when  $\alpha(t)$  is near a negative even integer,  $-2N$  say, the order of these polynomials will be  $N + N', 0$ , and  $3N + N'$ , respectively to within  $\pm 1$ , where  $N'$  denotes the number of real zeros of  $F(s,t)$  in the interval  $(0,t)$ .

#### Case (a)

Case (a) of our crossing symmetric model, has phase contours that differ from those in Fig. 2.1, by having an oscillatory phase in

the region  $u < 0, t < 0$ , giving phase contours  $\pi, \pi, \pi, \dots$ , in this region also. In addition the complex zeros (dotted lines in Fig. 2.1) go to infinity and leave the physical sheet at values  $t^1, t^2, t^3, \dots$ , which satisfy Eq. (2.2). Thus the real zeros shown in Fig. 2.1, become directly associated with the zeros of residues, in case (a).

The reduction of  $F$  to a Herglotz function, for fixed  $t$  in case (a), will give a form similar to that in Eq. (2.14), except that the order of the polynomials will now be 0, 0, and  $2N$  for  $P_a, P_b, P_c$ , respectively, to within  $\pm 1$ . In case (a) we take the real zeros to be in one to one correspondence with the zeros of residues, so that no more than one is on the physical sheet for each negative value of  $t$ .

Further discussion of cases (a) and (b) in the complex  $s$  plane for fixed negative  $t$  is given in II. The information obtained there about the complex phase contours is necessary for the above conclusions and the reader should refer especially to II Section 5 for further details.

## 3. PHASE CONTOURS AND FIXED ANGLE BEHAVIOR

At a fixed angle we cannot make direct deductions from our model, either about the spacing of phase contours, or about the location of zeros, since both would require detailed assumptions about the form of the Regge trajectories, and the way in which different terms interfere. Such assumptions may be essential for a more detailed treatment but they are not appropriate to the discussion of general features with which we are concerned here. Instead we will use consistency arguments, based on the assumption that the differential cross section at fixed angle falls like some entire function for large  $s$ . Thus,

$$F(s, \cos \theta) \sim B \exp[-A s^p], \quad (3.1)$$

where the order  $p$  and the type  $A$  both depend on  $\theta$ .

In case (b), discussed in II (Section 5 and 7) and in the previous section, the real phase contours are given by Fig. 2.1. At fixed angle, on our assumption of dominance by Regge terms having continuously falling trajectories as  $t$  decreases, the phase  $\phi(s, \cos \theta)$  increases continuously as  $s \rightarrow +\infty$  along  $s + i0$ , for real  $\cos \theta$  in  $(-1, 1)$ . Only for  $\cos \theta = \pm 1$  does the behavior change radically; then the phase tends to  $\frac{1}{2} \pi$ , as  $s \rightarrow +\infty$ . For fixed angle and negative  $s$ , along  $s + i0$ , the phase oscillates. Hence, from our discussion in I, and in Section 2 above, we would expect the rate of

-10-

decrease of the amplitude, as  $s \rightarrow +\infty$ , to be related to the increase of the phase. There may also be zeros in  $\text{Im } s > 0$ , but for case (b) it is consistent to assume they are finite in number, and for simplicity we assume there are none.

If the phase contours, for fixed  $\theta$ , along  $s$  real and positive, ceased to cycle through multiples of  $2\pi$  for  $s > s_0$ , for case (b) on the above assumptions, we would obtain

$$F(s, \cos \theta) = \frac{H(s, \cos \theta)}{P_c(s, \cos \theta)}, \quad (3.2)$$

analogous to (2.14), where  $P_c$  is a polynomial in  $s$  of order  $n_0$  where  $n_0\pi$  denotes the phase near  $s = s_0$ . However, in our model the phase does not have an upper bound as  $s \rightarrow +\infty$  at fixed angle of scattering, and heuristically we must therefore replace the form (3.2) by

$$F(s, \cos \theta) = \frac{H(s, \cos \theta)}{R(s, \cos \theta)}, \quad (3.3)$$

where  $H$  is Herglotz in  $s$ , and  $R$  denotes an entire function obtained by factoring out the zeros of  $\text{Im } F$  on the right hand cut in the complex  $s$  plane.

More generally, without the use of our generalized Regge model, if an amplitude  $F(s, \cos \theta)$  has (i) a bounded phase as  $s \rightarrow -\infty$ , (ii) a finite number of zeros in  $\text{Im } s > 0$ , and (iii) an unbounded increasing phase as  $s \rightarrow +\infty$ , it would have the form (3.3) modified by

including a polynomial in the numerator. Conversely, if (i) and (ii) hold, and we assume Eq. (3.1) on experimental grounds, we can deduce (iii).

The qualitative form of the phase contours of  $F(s, \cos \theta)$  in the  $s$  plane, can be deduced from Fig. 2.1, with the aid of an extrapolation from the fixed  $t$  phase contours considered in II (Section 5). They are shown in Fig. 3.1 for case (b). The order of the entire function  $R$  in Eq. (3.3) can be related to the asymptotic form of the phase contours on the left of Fig. 3.1, in the simple case where, for large  $|s|$  near  $\arg(s) = \pi$ ,

$$R(s, \cos \theta) \sim \exp[A|s|^p \exp(ip\psi)], \quad (3.4)$$

where  $\psi = \arg(s)$ . Then the phase contours have the asymptotic form

$$|s|^p \sin(p\psi) = \text{Constant}. \quad (3.5)$$

The order of  $R$  can also be related to the density of points at which  $\text{Im } F = 0$ , with  $\phi = n\pi$ , for large real and positive values of  $s$ . Let  $N(x)$  be the number of zeros of  $\text{Im } F(s, \cos \theta)$  for  $0 < s < x$ . From its construction (discussed in I Sections 2 and 4), the function  $R$  will have zeros at each of the real zeros of  $\text{Im } F$ , and  $N(x)$  will denote the number of zeros of  $R$  in  $|s| < x$ .

Jensen's theorem gives



$$\int_0^r \frac{N(x) dx}{x} = \frac{1}{2\pi} \int_0^{2\pi} [\log |R(r \exp i \psi)| d\psi] - \log[R(0)]. \quad (3.6)$$

R is of order  $p$ , so

$$\log |R(r \exp i \psi)| < K(\epsilon) r^{p+\epsilon}, \quad (3.7)$$

where  $\epsilon$  is any small positive number. Also,

$$\int_0^{2r} \frac{N(x) dx}{x} \geq N(r) \int_r^{2r} \frac{dx}{x} \geq N(r) \log 2. \quad (3.8)$$

Hence

$$N(r) \leq \frac{1}{\log 2} \int_0^{2r} \frac{N(x)}{x} dx < K r^{p+\epsilon}. \quad (3.9)$$

Thus the density of phase contours

$$\phi(s, t) = n\pi, \quad (3.10)$$

in Fig. 2.1, is closely related to the order  $p(\theta)$  of the entire function  $R$  for a fixed angle of scattering  $\theta$ .

In case (a), discussed in II (Sections 5 and 7) and in Section 2 above, the phase  $\phi(s, \cos \theta)$  has bounded oscillations along the real  $s$  axis above the branch cut. In this case the oscillations of  $\text{Im } F$  play only a minor role in the asymptotic behavior of  $|F|$ . If there were no zeros of  $F(s, \cos \theta)$  in  $\text{Im } s > 0$ , it would be

essentially a Herglotz function, and we would have an inequality like (2.13). This is in contradiction with our model which assumes dominance by leading Regge terms in the physical region. More generally it contradicts our requirement (3.1) for a rapid decrease of cross section at fixed angle.

We conclude that in case (a) there must be an infinite number of zeros of  $F(s, \cos \theta)$  in  $\text{Im } s > 0$ , when  $\cos \theta$  is in  $(-1, 1)$ , but  $\cos \theta \neq \pm 1$ . If the number of zeros was only finite, they would lead to a polynomial factor in  $F(s, \cos \theta)$ , like  $P_a(s)$  in Eq. (2.14), which would increase the power behavior at infinity. However, an infinite number of zeros, leads to an entire function, and we obtain

$$F(s, \cos \theta) = E(s, \cos \theta) H(s, \cos \theta), \quad (3.11)$$

where  $E$  is an entire function in  $s$ .

The zeros of  $F(s, \cos \theta)$  are evidently closely related to the zeros of residues in our model. They must all leave the physical sheet in the limits  $\cos \theta = \pm 1$ . For  $\cos \theta$  near to 1, say

$$\cos \theta = 1 - \epsilon, \quad (3.12)$$

we can discuss the location of the zero of  $F$  that is associated with a zero of a residue, as was done for fixed real  $t$  in II Section 5.

The leading Regge term  $F_1$ , and the next term  $F_2$ , give

$$F(s, t) \sim F_1 + F_2 = F_2 \left[ \frac{F_1}{F_2} + 1 \right], \quad (3.13)$$

-14-

for large  $s = s_0 \exp(i\psi)$ , where

$$\frac{F_1}{F_2} = \frac{\beta_1(t)}{\beta_2(t)} s_0^{(\alpha_1 - \alpha_2)} \exp \left[ i(\alpha_2 - \alpha_1) \left( \frac{1}{2} \pi - \psi \right) \right]. \quad (3.14)$$

From (3.12),

$$t \approx -\frac{1}{2} \epsilon s_0 \exp(i\psi). \quad (3.15)$$

We choose  $\epsilon$  to be small, then choose  $s_0$  large enough so that

$$-\frac{1}{2} \epsilon s_0 = t_1^0 - \epsilon', \quad (3.16)$$

where

$$\beta_1(t_1^0) = 0. \quad (3.17)$$

For  $t$  near  $t_1^0$ ,  $\beta_2$  is negative. For  $t > t_1^0$ ,  $\beta_1$  is positive, and for  $t < t_1^0$ ,  $\beta_1$  is negative. For simplicity, we take

$(\alpha_1 - \alpha_2) = 1$ . For  $\psi = 0$  in Eq. (3.14), the ratio  $F_1$  to  $F_2$

is pure imaginary. But for  $\psi > 0$ , from (3.15-17),  $\beta_1(t)$  will

become nearly pure imaginary even for small  $\psi$ , provided  $\epsilon'$  is

sufficiently small. The phase of  $\beta_1$  will then cancel the phase

from the exponential in Eq. (3.14). Since  $\beta_2$  is negative, we obtain

$$\frac{F_1}{F_2} \approx -\frac{(\epsilon s_0 \psi) s_0}{2|\beta_2|}. \quad (3.18)$$

We can choose  $\psi$  so that this ratio is a minus one, giving a zero in (3.13). As  $\epsilon \rightarrow 0$ , this zero of  $F(s, \cos \theta)$  tends to infinity in the  $s$  plane, just above the real axis.

The phase contours and zeros of  $F(s, \cos \theta)$ , for complex  $s$ , are shown in Fig. 3.2 for case (a). Since  $F$  is real analytic, the phase contours and zeros on the physical sheet in  $\text{Im } s < 0$  will be the mirror image of those shown in  $\text{Im } s > 0$ .

It is evident from Figs. 3.1 and 3.2 that their essential features are closely related. In Fig. 3.1 the zeros lie on the unphysical sheet through the right hand branch cut. When one changes from case (b) [Fig. 3.1] to case (a) [Fig. 3.2] the zeros simply lift up from the unphysical sheet on to the physical sheet.

The actual behavior of phase contours and zeros is likely to be a mixture of case (b) and case (a). Then we would expect the high energy behavior at fixed angles to depend on the ratio of entire functions giving,

$$F(s, \cos \theta) = \frac{E(s, \cos \theta) L(s, \cos \theta) H(s, \cos \theta)}{R(s, \cos \theta)}, \quad (3.19)$$

where  $L(s, \cos \theta)$  comes from real values of  $s$  where  $\text{Im } F(s, \cos \theta) = 0$ , at which the phase  $\phi$  is decreasing.  $R$  comes from similar values where  $\phi$  is increasing.  $E$  comes from the zeros of  $F$ , on the physical sheet.

If the entire function  $E$  is dominant for large  $s$ , then its order must be greater than or equal to  $\frac{1}{2}$ . This follows from Polya's

inequality, which states that

$$m(r) \geq [M(r)]^{\{\cos(p \pi) - \epsilon\}}, \text{ for large } r, \quad (3.20)$$

where  $m(r)$  and  $M(r)$  denote the minimum and maximum values of the entire function on  $|s| = r$ , and  $p$  denotes its order. In defining  $m(r)$  the neighborhoods of zeros are excluded. Thus, if  $p$  was less than  $1/2$ , we could deduce that  $m(r)$  increases with  $r$ , and the differential cross section would increase with energy at fixed angle. We reject this on physical grounds and deduce that the order  $p$  satisfies

$$p \geq \frac{1}{2}. \quad (3.21)$$

If a smooth angular dependence is assumed, we can also reject  $p < \frac{1}{2}$  on the grounds that it contradicts unitarity.

## 4. MODULUS CONTOURS AT HIGH ENERGY

A fixed angle lower bound was first obtained by Cerulus and Martin<sup>3</sup> under certain assumed uniform boundedness properties of the scattering amplitude. Their results were generalized by Chiu and Tan,<sup>4</sup> who discussed also their relation to rising Regge trajectories. Using analagous methods but different assumptions, Tiktopoulos and Treiman<sup>5</sup> have obtained certain constraints on the angular dependence of scattering amplitudes.

In this section we discuss the characteristic features of phase contours in the  $z_t$  plane at large values of  $t$ , where  $t$  denotes the energy and  $z_t$  the cosine of the scattering angle. Using the harmonic properties of the phase and modulus contours we note how one can define a region  $D_\infty$  in the  $z_t$  plane, in which the scattering amplitude is polynomial bounded. The properties of the region  $D_\infty$  are used in Section 5 to provide a lower bound for fixed angle behavior that is a generalization of earlier results.

In formulating our approach we make use of our deductions about phase contours for the crossing symmetric model developed in II and discussed in previous sections. Some of our conclusions are more general in character and depend only on the specific asymptotic form of certain modulus contours.

(a) Phase Contours in the  $z_t$  Plane

For fixed  $t$ , the transformation from  $s$  to  $z_t$  is linear, so the topology of the phase contours will not be altered in going from the  $s$  plane to the complex  $z_t$  plane,

$$z_t = 1 + \frac{2s}{t - 4m^2} = \frac{s - u}{t - 4m^2}. \quad (4.1)$$

We consider the phase contours for real  $t$  above the branch cut  $(t + i0)$ , in the complex  $z_t$  plane. These are analogous to those shown in paper II Fig. 7.2. Using the limit  $t + i0$ , the real section for  $t > 4m^2$  differs from that shown in Fig. 2.1 by (i) an interchange of the left hand side with the right hand side, and (ii) the  $3\pi/2$  contours are replaced by  $\pi/2$  contours. The resulting complex section is shown in the  $z_t$  plane in Fig. 4.1, for real  $t$  corresponding to

$$3 < \alpha(t) < 4. \quad (4.2)$$

The asymptotic phase in the  $z_t$  plane is given by

$$\phi(t + i0, z_t) \sim \frac{1}{2} \pi + \alpha(t)\theta, \quad (4.3)$$

where  $z_t = |z_t| \exp(i\theta)$ , and  $z_t \rightarrow \infty$ , for  $0 \leq \theta \leq \pi$ . This corresponds to asymptotic behavior  $|z_t|^{\alpha(t)}$  of the modulus of  $F$ ,

-19-

for large  $|z_t|$ . Note that the region above the right hand cut in the  $z_t$  plane corresponds to  $\text{Im}(s) > 0$ , whereas that above the left hand cut corresponds to  $\text{Im}(u) < 0$ . This explains the asymmetry since  $t$  also is above threshold. In addition there is no real region where the amplitude  $F$  is also real (because  $t > 4m^2$ ), so we do not have any upper and lower half-plane symmetry.

In our model we assume that as  $t$  increases  $\alpha(t)$  increases without limit. Then, for increasing  $t$ , there will be new phase contours continuously entering the physical sheet of the  $z_t$  plane from the left hand cut. All of these contours remain unbounded (i. e. they go to infinity) on the physical sheet.

In contrast to the phase contours from the left hand cut, there will be a class of bounded contours coming from the region

$$-1 - \frac{8m^2}{t - 4m^2} < z_t < 1 + \frac{8m^2}{t - 4m^2} \quad (4.4)$$

These contours are associated with decreasing  $\alpha(s)$  and  $\alpha(u)$  in the physical  $t$  channel, as  $s$  and  $u$  became more negative.

The above unbounded and bounded types of contours are separated by the leading bounded  $\pi$  contour. In addition, there are  $\frac{1}{2} \pi$  contours associated with the right hand cut, but our argument does not require us to know whether these are unbounded or bounded. We denote by  $\Delta_t$  the region in the  $z_t$  plane that is bounded by the leading  $\pi$  contour for given  $t$ .



As  $t \rightarrow +\infty$ , the phase contours in the real  $(s, t, u)$  plane become parallel to  $u = \text{constant}$ , or  $s = \text{constant}$ . Thus a particular phase contour, say

$$\phi(t, z_t) = \frac{1}{2} \pi + n\pi, \quad (4.5)$$

will meet the left hand cut of the  $z_t$  plane at a point  $P_n$  given by,

$$z_t = -1 - \frac{2c(n)}{t - 4m^2}, \quad (4.6)$$

where  $c(n)$  is defined by

$$\alpha[c(n)] = n. \quad (4.7)$$

The phase (4.5) using (4.6) will apply out to the point A in Fig. 4.1, where the phase contour through the sequence of zeros meets the real  $z_t$  axis. As  $t \rightarrow +\infty$ , the point A in our model tends to  $z_t = -3$ , since it lies on the line  $u = t$ . In contrast, each point  $P_n$ , for fixed  $n$ , will approach  $z_t = -1$  as  $t \rightarrow +\infty$ , like  $(t)^{-1}$ . The phase contours (4.5) will wind around the bounded  $\pi$  contour, and then move to infinity in their asymptotic direction in the  $z_t$  plane, found from Eq. (3.4). At the same time, for increasing  $t$ , the bounded phase contours will become denser near the limiting  $\pi$  contour, within the region  $\Delta_t$  that it bounds.

We will assume that as  $t \rightarrow +\infty$ ,

$$\Delta_t \rightarrow \Delta_\infty, \quad (4.8)$$

where  $\Delta_\infty$  is a finite bounded region in the  $z_t$  plane. For simplicity, we assume that

$$\Delta_{t_1} \subset \Delta_{t_2}, \quad \text{if } t_1 < t_2. \quad (4.9)$$

Then all of the closed phase contours, for finite  $t$ , lie inside  $\Delta_\infty$ .

The general form of the phase contours for large  $t$  is sketched in Fig. 4.2. As noted above, we do not expect these contours to show any symmetry with respect to  $\text{Im}(z_t) = 0$ . In particular the boundary of  $\Delta_t$  will not in general meet the real axis at right angles. We denote the angles by  $\theta_1(t)$  and  $\theta_2(t)$  as shown in Fig. 4.2, and assume that they tend to values  $\theta_1$  and  $\theta_2$  in  $(0, \frac{1}{2}\pi)$  as  $t \rightarrow \infty$ .

#### (b) Modulus Contours in the $z_t$ Plane

The phase  $\phi(s, t)$ , and  $\log|F(s, t)|$ , are respectively the imaginary and the real parts of  $\log[F(s, t)]$ . Hence they are harmonic functions of  $x$  and  $y$ , where  $z_t = x + iy$ . From the properties of harmonic functions, the phase contours and the modulus contours will be mutually orthogonal in the complex  $z_t$  plane. If the phase contours are known, the modulus contours can be constructed. For example,

if  $|z_t|$  is large enough, the modulus contours will approximate to semicircles centered on the origin with radius  $|z_t|$ . The phase and modulus contours, that correspond to fixed real  $t$  such that  $3 < \alpha(t) < 4$ , are shown in Fig. 4.3

We will make special use of the modulus contour that goes through the thresholds at  $z_t = \pm\rho$ , where

$$\rho = 1 + \frac{8m^2}{t - 4m^2}. \quad (4.10)$$

This contour is given by

$$|F(t, z_t)| = |F(t, \rho)|, \quad (4.11)$$

and we will denote the corresponding curve in the  $z_t$  plane by  $\Gamma_t$ . Its shape will change as  $t$  is increased, and its detailed form will depend on the dynamics of the system. For our model, we expect it to approach the form  $\Gamma_\infty$ , that is indicated in Fig. 4.4, enclosing an area  $D_\infty$  in the  $z_t$  plane. We expect  $D_\infty$  to enclose  $\Delta_\infty$ , since the modulus contours are orthogonal to the phase contours. In general the angle  $\delta$  of  $\Gamma_\infty$  with the left hand real axis will differ from the corresponding angle with the right hand axis.

For  $z_t^i$  inside  $D_\infty$  in the  $z_t$  plane, we will have

$$\frac{F(t, z_t^i)}{t^2} \rightarrow 0, \quad \text{as } t \rightarrow \infty, \quad (4.12)$$

since for large  $t$ ,

$$|F(t, \pi)| < t^{2-\epsilon}. \quad (4.13)$$

Outside  $D_\infty$ , in our model, any modulus contour  $\Gamma_t(n)$ , having a value  $t^n$  (with  $n$  fixed), will move towards  $\Gamma_\infty$  and will coincide with it in the limit  $t \rightarrow \infty$ . Hence at any fixed point  $z_t^0$  outside  $D_\infty$ , we will have

$$\frac{F(t, z_t^0)}{t^n} \rightarrow \infty, \text{ as } t \rightarrow \infty. \quad (4.14)$$

Thus, in our model, the modulus of the amplitude will be bounded by a polynomial in  $t$  as  $t \rightarrow \infty$ , for points  $z_t^i$  inside  $D_\infty$ . It will not be bounded by a polynomial for points  $z_t^0$  outside  $D_\infty$  in the  $z_t$  plane. This suggests a need for new generalization of the results of Cerulus and Martin<sup>3</sup> on a fixed angle bound. Our generalization, which we give in the next section does not depend on the special assumptions involved in our model. However it is designed to take into account the special features and difficulties that the model indicates are likely to be associated with rising Regge trajectories, or more generally with scattering amplitudes that are not polynomial bounded.

## 5. A FIXED ANGLE LOWER BOUND

In the general case we assume that, for any  $t$ , there exists a region  $D_t$  of the  $z_t$  plane, within which the amplitude is polynomial bounded in the variable  $t$ . We assume that as  $t \rightarrow \infty$ ,  $D_t$  has the limiting form shown as  $D$  in Fig. 4.4, and makes an angle  $\delta$  with the left hand (and right hand) branch cuts. Let  $\Gamma_t$  be the boundary curve of  $D_t$ . As noted by Chiu and Tan,<sup>4</sup> the method of Cerulus and Martin<sup>3</sup> requires  $\delta = 0$ , whereas we would in general expect  $\delta$  to be non-zero.

We will make a transformation such that the image of the curve  $\Gamma_t$  becomes tangential to the real axis at the image of the points  $z_t = \pm\rho$ . Once this is done, we can then use the Cerulus-Martin theorem<sup>6</sup> to obtain a lower bound at fixed angle as  $t \rightarrow \infty$ . A transformation satisfying this requirement is given by,

$$w(z_t) = \frac{\left[ \rho^{4\alpha} - (\rho^2 - z_t^2)^{2\alpha} \right]^{\frac{1}{2}}}{\left[ \rho^{4\alpha} - (\rho^2 - 1)^{2\alpha} \right]^{\frac{1}{2}}}, \quad (5.1)$$

where

$$\frac{1}{2\alpha} = 1 - \frac{\delta}{\pi}. \quad (5.2)$$

The appropriate branch of  $w$  is the one whose inverse

$$z_t = \left[ \rho^2 - \left\{ \rho^{4\alpha} - \left[ \rho^{4\alpha} - (\rho^2 - 1)^{2\alpha} \right] w^2 \right\}^{\frac{1}{2\alpha}} \right]^{\frac{1}{2}}, \quad (5.3)$$

is real analytic and Herglotz.

Consider the function

$$G(t, w) \equiv F(t, z_t). \quad (5.4)$$

It has branch points at

$$w_\rho = \pm \frac{\rho^{2\alpha}}{\left[\rho^{4\alpha} - (\rho^2 - 1)^{2\alpha}\right]^{\frac{1}{2}}}, \quad (5.5)$$

and as  $t \rightarrow \infty$ ,

$$w_\rho \sim 1 + \frac{C}{t^{2\alpha}}. \quad (5.6)$$

With the usual assumptions,<sup>3,4</sup> which include a specification of the form of  $D_t$ , we can apply the Cerulus Martin theorem and find that

$$|F(t, z_t)| \geq C' \exp[-C_\alpha(z_t) t^\alpha \log t]. \quad (5.7)$$

for  $-1 \leq z_t \leq 1$ , as  $t \rightarrow \infty$ . If we assume

$$0 \leq \delta < \frac{1}{2} \pi (1 - \epsilon), \quad (5.8)$$

we obtain

$$\frac{1}{2} \leq \alpha < \frac{1}{1 + \epsilon}. \quad (5.9)$$

#### ACKNOWLEDGMENT

We are indebted for hospitality and for helpful discussions to Professor G. F. Chew at the Lawrence Radiation Laboratory, Berkeley.

## FOOTNOTES AND REFERENCES

- \* This work was supported by the United States Atomic Energy Commission.
- † Now at the Cavendish Laboratory, Cambridge, England.
1. C. B. Chiu, R. J. Eden and C-I Tan, "Phase Contours of Scattering Amplitudes I, Phase Contours, Zeros and High Energy Behavior", UCRL-17899 (1967). This paper is denoted I in the text.
  2. R. J. Eden and C-I Tan, "Phase Contours of Scattering Amplitudes II, Crossing Symmetry, Resonance Poles and High Energy Behavior", UCRL-17922 (1967). This paper is denoted II in the text.
  3. F. Cerulus and A. Martin, Phys. Lett. 8, 80 (1964).
  4. C. B. Chiu and C-I Tan, Phys. Rev. 162, 1701 (1967).
  5. G. Tiktopoulos and S. B. Treiman, Angular Dependence of Scattering at High Energies (Princeton preprint 1967).
  6. This is a generalization of the theorem proved by Cerulus and Martin which was given in Ref. 4 by Chiu and Tan. Note a minor difference between the case here and that in Ref. 4. There the function has only a right hand cut, whereas here it has both right and left hand cuts. Consequently the bound here is slightly weaker, but the assumptions also are weaker.

## FIGURE CAPTIONS

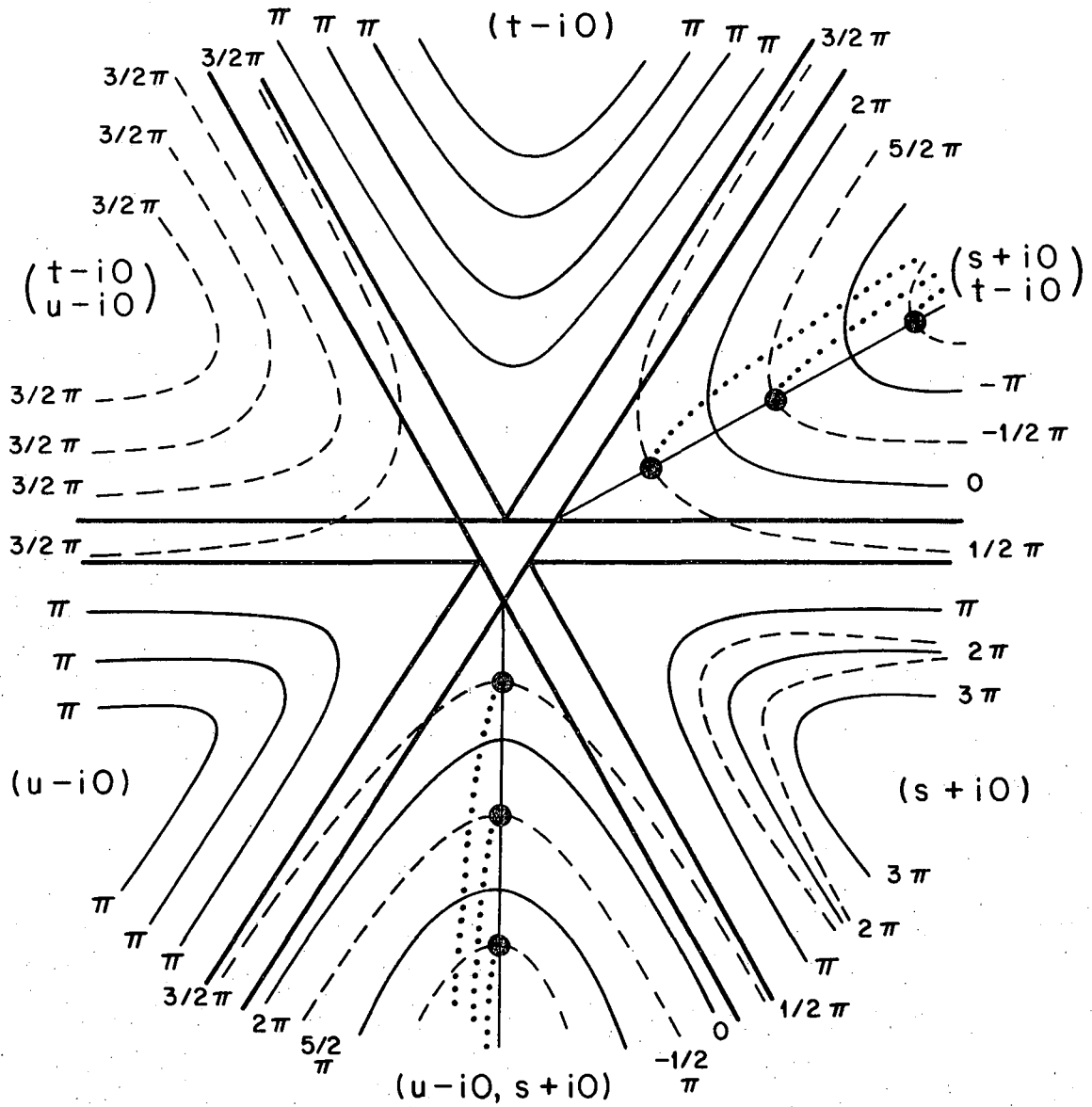
- Fig. 2.1. Phase contours in the real  $(s, t, u)$  plane, for a crossing symmetric amplitude based on the generalized Regge model. The small black circles indicate real zeros and the dotted lines indicate complex zeros. The phase contours and zeros correspond to case (b) discussed in the text.
- Fig. 3.1. Phase contours in the complex  $s$  plane for fixed angle in case (b). This complex section corresponds to the phase contours shown in Fig. 2.1 for real  $s$  and  $t$ .
- Fig. 3.2. Phase contours and zeros in the complex  $s$  plane for fixed angle in case (a). The zeros are shown as small black circles, at the intersections of phase contours for which  $\text{Im } F = 0$  and phase contours for which  $\text{Re } F = 0$ .
- Fig. 4.1. Phase contours in the complex  $z_t$  plane for  $t$  real in the limit  $(t + i0)$ , such that  $3 < \alpha(t) < 4$  in the crossing symmetric model. The upper phases are obtained for a path above the zeros, the lower phases are for a path below the zeros, in both cases starting from the real axis on the right hand side.



Fig. 4.2. Phase contours in the  $z_t$  plane in the crossing symmetric model for large energy ( $t$ ).

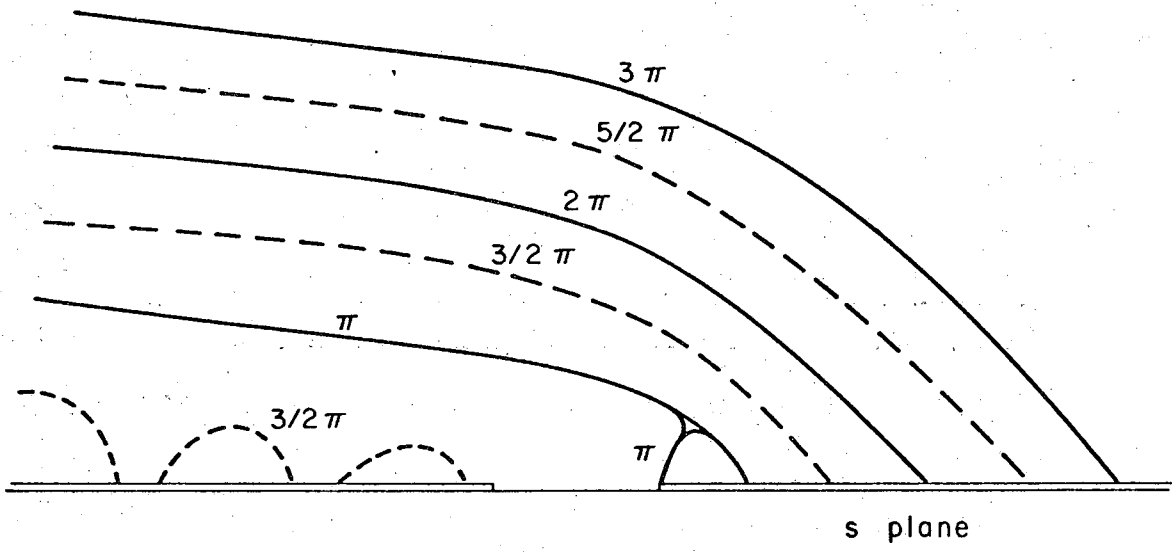
Fig. 4.3. Phase contours (heavy lines) and modulus contours (thin lines) for the crossing symmetric model, in the complex  $z_t$  plane. The energy has similar value to that giving the phase contours in Fig. 4.1.

Fig. 4.4. The asymptotic limit  $\Gamma_{\infty}$  of modulus contours that correspond to a polynomial in the energy ( $t$ ), shown in the  $z_t$  plane. The interior of  $\Gamma_{\infty}$  is the region denoted  $D_{\infty}$ . The curve  $\Gamma$  is symmetric and within  $D_{\infty}$ , it surrounds the region  $D$ .



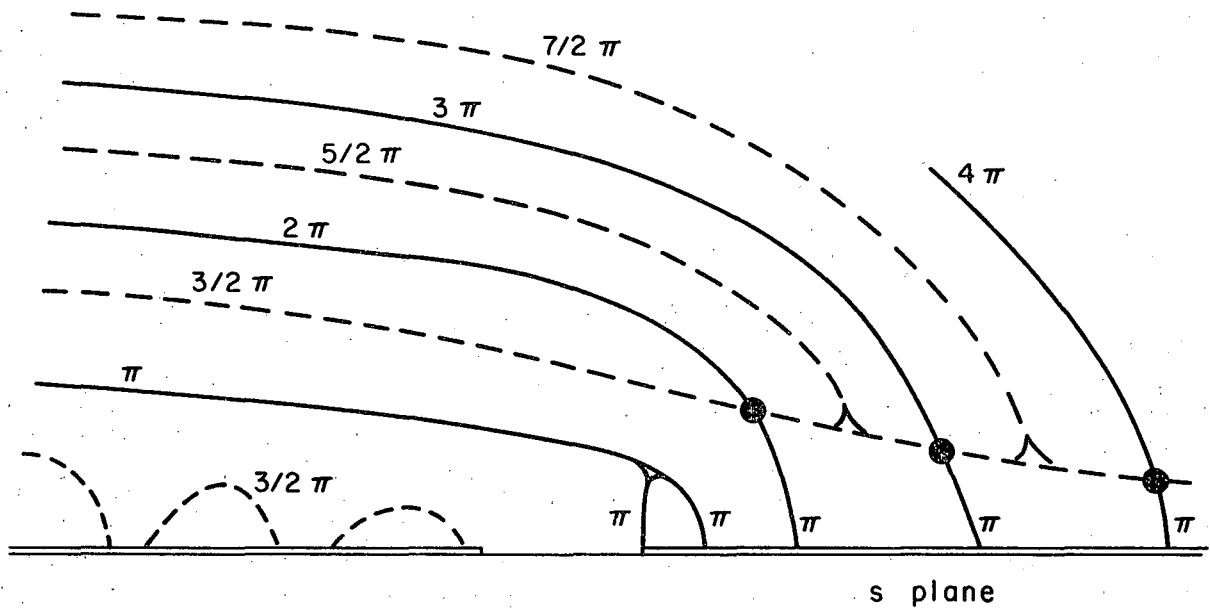
XBL6711-5570

Fig. 2.1



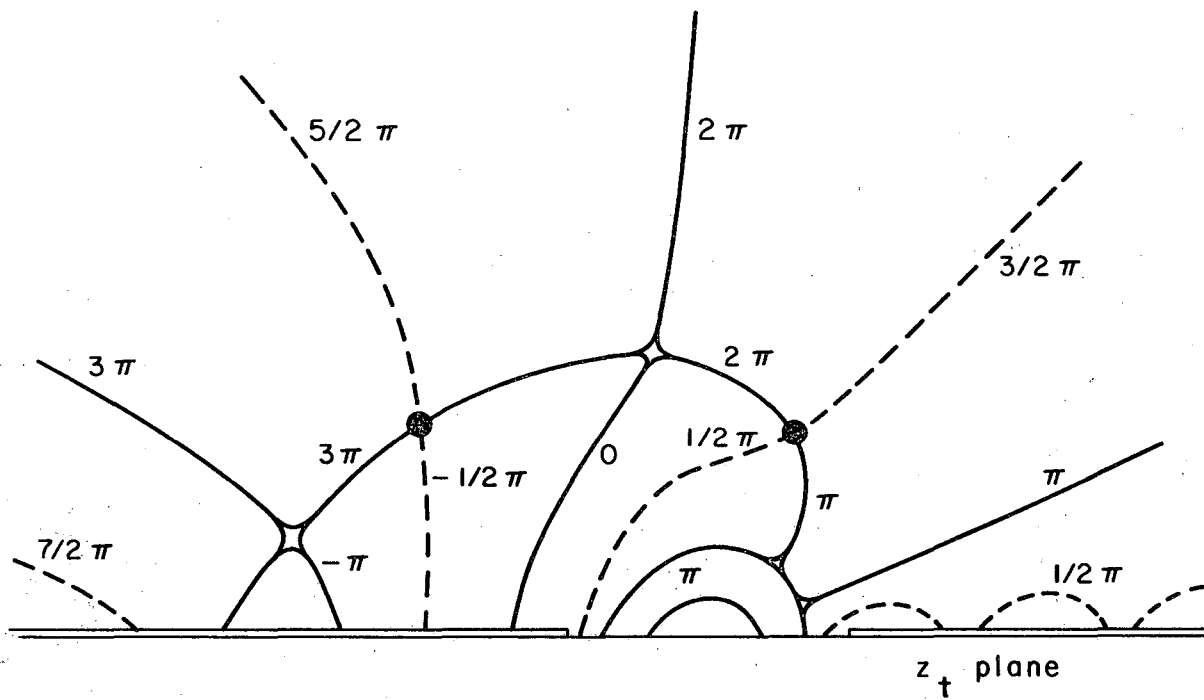
XBL681-1506

Fig. 3.1



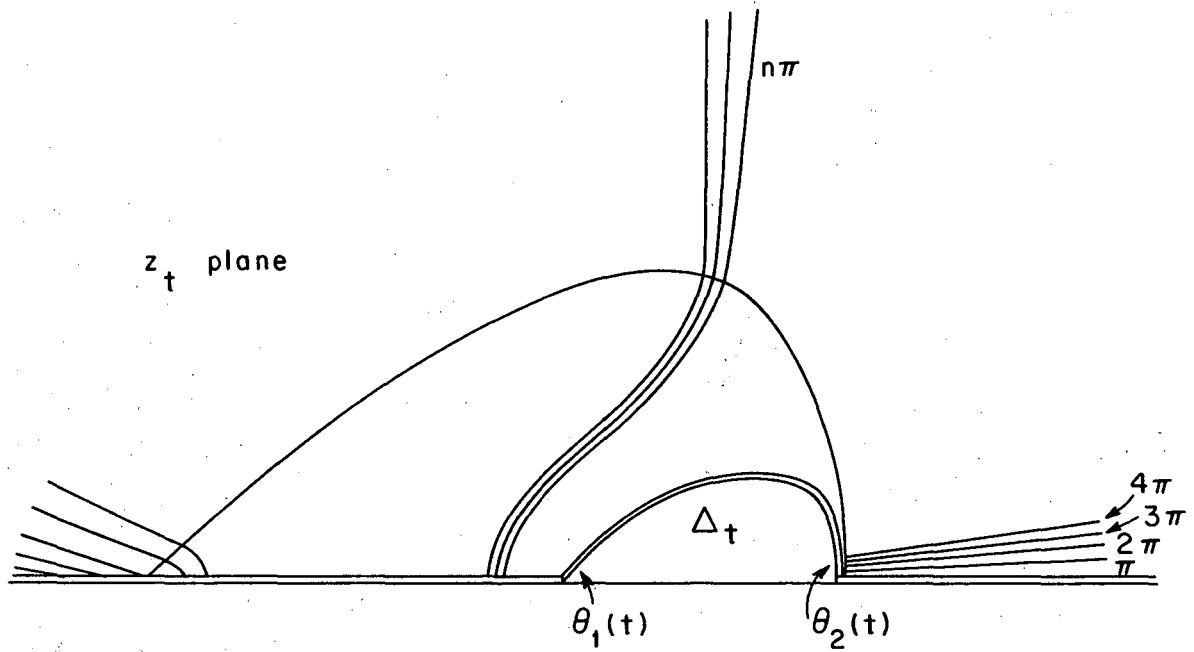
XBL681-1507

Fig. 3.2



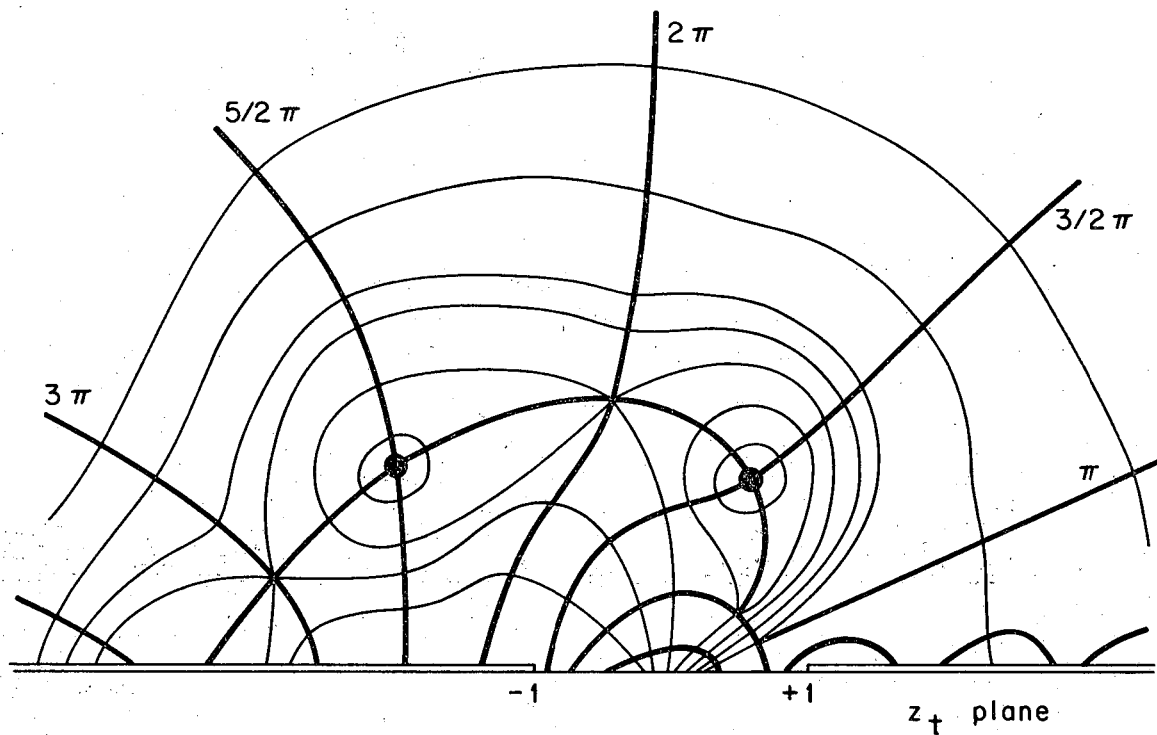
XBL681-1508

Fig. 4.1



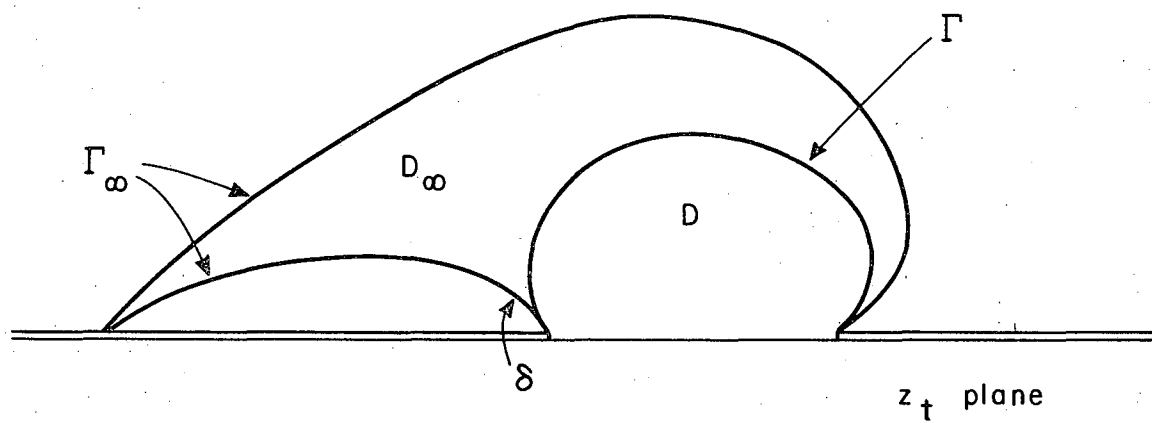
XBL681-1509

Fig. 4.2



XBL681-1510

Fig. 4.3



XBL681-1511

Fig. 4.4



This report was prepared as an account of Government sponsored work. Neither the United States, nor the Commission, nor any person acting on behalf of the Commission:

- A. Makes any warranty or representation, expressed or implied, with respect to the accuracy, completeness, or usefulness of the information contained in this report, or that the use of any information, apparatus, method, or process disclosed in this report may not infringe privately owned rights; or
- B. Assumes any liabilities with respect to the use of, or for damages resulting from the use of any information, apparatus, method, or process disclosed in this report.

As used in the above, "person acting on behalf of the Commission" includes any employee or contractor of the Commission, or employee of such contractor, to the extent that such employee or contractor of the Commission, or employee of such contractor prepares, disseminates, or provides access to, any information pursuant to his employment or contract with the Commission, or his employment with such contractor.

